Published in final edited form as:
Nat Med. 2009 November ; 15(11): 1298–1306. doi:10.1038/nm.2052.

Activation of PKCδ and SHP1 by hyperglycemia causes vascular cell apoptosis and diabetic retinopathy

Pedro Geraldes[1], **Junko Hiraoka-Yamamoto**[1], **Motonobu Matsumoto**[1], **Allen Clermont**[1], **Michael Leitges**[3], **Andre Marette**[4], **Lloyd P Aiello**[1,2,7], **Timothy S Kern**[5], and **George L King**[1,6]

[1]Dianne Nunnally Hoppes Laboratory for Diabetes Complications, University of Oslo, Oslo, Norway

[2]Beetham Eye Institute, University of Oslo, Oslo, Norway

[3]Joslin Diabetes Center, University of Oslo, Oslo, Norway

[4]Department of anatomy and physiology, Université Laval, Québec, Canada

[5]Department of Medicine, Case Western Reserve University, Cleveland, OH

[6]Department of Medicine, Harvard Medical School, Boston, MA, USA

[7]Department of Ophthalmology, Harvard Medical School, Boston, MA, USA

Abstract

Cellular apoptosis induced by hyperglycemia occurs in many vascular cells and is critical to initiate diabetic pathologies. In the retina, pericyte apoptosis, the most specific vascular pathology attributed to hyperglycemia, is linked to the loss of PDGF actions due to unknown mechanisms. Our study demonstrated that hyperglycemia persistently activated PKCδ and p38α MAPK to increase the expression of a novel target, SHP-1, leading to PDGF receptor-β dephosphorylation and actions, and increased pericyte apoptosis, independent of NF-κB. These findings were also observed in diabetic mouse retinas, which were not reversed by achieving normoglycemia with insulin. Unlike diabetic controls, diabetic *Prkcd*$^{-/-}$ mice did not exhibit p38α MAPK/SHP-1 activation, PDGF resistance or acellular capillaries. Since PKCδ/p38α MAPK/SHP-1 activation are also induced in the brain pericytes and renal cortex by diabetes, these findings have elucidated a new pathway by which hyperglycemia can induce PDGF resistance and increase vascular cell apoptosis to cause diabetic vascular complications.

A common cellular pathology for many diabetic vascular complications is an enhanced rate of cellular apoptosis as observed in retinal pericytes, renal podocytes and vascular endothelial cells (EC). [1, 2] Hyperglycemia, the major risk factor for diabetic microvascular complications, [3] is responsible for inducing apoptosis in these vascular tissues directly [4] or indirectly [5, 6] from alteration of cytokines and toxic product accumulation in diabetes. Although intensive insulin treatment in diabetic patients can delay the onset and progression

Address correspondence to: George L. King, MD, Joslin Diabetes Center, One Joslin Place, Boston, MA 02215, USA Tel.: 617-732-2622; Fax: 617-732-2637 george.king@joslin.harvard.edu.

AUTHOR CONTRIBUTIONS

P.G. and G.L.K. have conceived, designed and performed most of the research, analyzed the data and wrote the manuscript. J.H-Y and M.M. have conducted the research experiments using the laser micro-dissection and rat studies. A.C. has performed the RBF and MCT studies. M.L. has provided the Prkcd$^{-/-}$ mice. A.M. has provided the adenoviral vector dominant negative of SHP-1. L.P.A. has conceived and edited the manuscript. T.S.K. has performed the acellular capillaries and pericytes loss measurements, analyzed the data and edit the manuscript.

of diabetic complications, [3] initiation of intensive glycemic control after periods of poor glycemia did not decrease the rate of progression of retinopathy and other microvascular diseases significantly, suggesting hyperglycemia-induced chronic cellular changes are difficult to reverse. [7] To clarify the biochemical mechanisms involved in hyperglycemia-induced cellular apoptosis, we characterized the signaling cascade of hyperglycemia leading to pericyte apoptosis in diabetic retinopathy (DR), the most specific vascular pathology attributed to diabetes, which may represent a common pathway for other microvascular abnormalities in diabetes. [8, 9] One of the most interesting recent findings related to pericyte apoptosis is the role of platelet derived growth factor receptor-β (PDGFR-β). PDGF-B/PDGFR-β deficient mice displayed retinal pericyte depletion with parallel formation of microaneurysms and acellular capillaries recapitulating the early changes of DR. [10] However, it is unclear whether pericyte loss results from decreases in PDGF-B levels, since the expression of PDGF-B in the retina of diabetic rats is increased. [11] In addition, although oxidative stress and activation of the nuclear factor-kappa B (NF-κB) have been reported to be involved in hyperglycemia-induced cell death, the interrelationship of PDGF-B inhibition and oxidative stress in mediating pericyte apoptosis and initiation of diabetic retinopathy is not known. We discovered that hyperglycemia can activate protein kinase C δ (PKCδ) and p38α MAPK, increasing the expression of a protein tyrosine phosphatase (PTP), Scr homology-2 domain containing phosphatase-1 (SHP-1), which in turn leads to the dephosphorylation of PDGFR-β both in culture cells and *in vivo* models of diabetes. SHP-1 negatively regulates multiple tyrosine receptor pathways, including PDGF, and insulin receptors. [12, 13] However, the ability of PKCδ/p38αMAPK to activate SHP-1 and the effects of SHP-1 to cause pericyte apoptosis and DR is not known.

RESULTS

PKCδ on PDGF resistance and acellular capillary formation

Since PKC activation is associated with retinal and vascular pathologies of diabetes [14], we studied the effects of PKC activation on PDGF resistance and pericyte apoptosis. *In situ* PKC activity increased by 40% ($P = 0.028$) in mouse retina after three months of diabetes (Fig. 1a). Immunoblot analyses showed that both PKCβ2 and PKCδ isoform ($P = 0.022$ and $P = 0.043$) were increased in the membrane fractions of isolated retinal microvessels (Fig. 1b) and the whole retina (Supplementary Fig. 1a online). PKCδ activation induces apoptosis in other cell types. [15] Therefore, retinal vascular changes in non-diabetic (NDM) and diabetic (DM) PKCδ null ($Prkcd^{-/-}$) and age-matched control ($Prkcd^{+/+}$) mice were evaluated after 6 months of duration with or without interventional glycemic control with insulin implants (Supplementary Fig. 1b online). After 6 months, $Prkcd^{+/+}$ and $Prkcd^{-/-}$ DM mice had lower body weight and plasma insulin levels, but increased glucose concentration compared with NDM mice with similar genetic background. Diabetic mice treated with insulin implants gained weight, normalized glucose level for the last 3 months but had hyperinsulinemia (Supplementary Table 1 online). Histological analyses of the retina demonstrated that diabetes increased acellular capillaries (red arrows) by 59% ($P < 0.05$) (Fig. 1c) or acellular capillaries + pericyte ghosts or strands (Supplementary Fig. 1c,d online) as compared to NDM $Prkcd^{+/+}$ mice but not in DM $Prkcd^{-/-}$. The reduction in blood glucose for the last 3 months did not prevent the onset of acellular capillaries.

In the retina, the conditional endothelial PDGF-B deficient mice exhibited pericyte loss, microaneurysm formation and acellular capillaries. [10] Thus, we evaluated the ability of PDGF-BB to activate ERK and Akt in the retina with PKCδ activation. After intravitreous injection of PDGF-BB, levels of phospho-ERK and -Akt in the retina of NDM $Prkcd^{+/+}$, NDM and DM $Prkcd^{-/-}$ mice increased by 1.6 to 2.1-fold ($P < 0.05$), but unchanged in DM $Prkcd^{+/+}$ mice (Fig. 1d). VEGF, PDGF-B, PKCβ and PKCδ mRNA or protein expression increased in isolated retinal microvessels (Fig. 1e,f) and in whole retina (Supplementary Fig.

2a–c online) of DM as compared with NDM *Prkcd*$^{+/+}$ mice by 2.4 to 2.9-fold ($0.001 < P < 0.05$). Normalization of blood glucose did not prevent the increases in PDGF-B or PKCδ protein or mRNA expression induced by diabetes (Supplementary Fig. 2a–c online). Consistent with the histological retinal findings, PDGF-B, PKCβ and VEGF protein and mRNA expression were not increased in DM *Prkcd*$^{-/-}$ mice as compared to NDM *Prkcd*$^{-/-}$ mice (Fig. 1e,f, Supplementary Fig. 2a-c online). Moreover, phosphorylation of PKCδ (tyrosine 311) was increased in DM as compared with NDM *Prkcd*$^{+/+}$ mice, confirming activation of PKCδ isoform in retina of diabetic animals (Supplementary Fig. 2a online). Flat mount retina injected with FITC-dextran and Evans blue showed increased leakage and permeability ($P = 0.038$) in DM as compared with NDM *Prkcd*$^{+/+}$ mice but not in DM *Prkcd*$^{-/-}$ mice (Fig. 1G). Mice with 4 weeks of diabetes had a 46% reduction of RBF ($P < 0.05$) and a 78% increase in MCT ($P < 0.01$) as compared to NDM *Prkcd*$^{+/+}$ mice (Supplementary Fig. 3a,b online). Interestingly, DM PKCδ$^{-/-}$ mice also exhibited a decrease in RBF and an increase in MCT versus NDM *Prkcd*$^{-/-}$ mice (Supplementary Fig 3a,b online). Alteration of RBF in mice by hyperglycemia appears to be transient since our data showed that blood flow returned to basal level after 2 months duration of diabetes (Supplementary Fig. 3c online). In addition, transgenic ET-1 promoter mice displayed decreased RBF (Supplementary Fig. 3d online), but they did not develop vascular pathologies even after 12 months of life.

HG induced pericyte apoptosis and PDGF-B actions by PKCδ

To identify the mechanisms by which glucose levels and PKCδ isoform activation may inhibit PDGF-B action and increase pericyte apoptosis, we developed a cultured bovine retinal pericytes (BRPC) model that mimics the chronic effects of hyperglycemia on retinal pericyte pathology (Supplementary Fig. 4a online). Exposure to HG for 72 hours increased DNA fragmentation by 2-fold ($P < 0.01$) and annexin V marker by 11.7% as compared to LG condition (Fig. 2a and Supplementary Fig. 4b online). Decreasing glucose from HG to LG for an additional period of 3 days did not prevent pericyte apoptosis (Fig. 2a). Stimulation with PDGF-BB decreased DNA fragmentation by 31% ($P < 0.05$) in LG condition. However, PDGF-BB did not prevent HG-induced DNA fragmentation even after reducing to LG level for 3 more days (Fig. 2a). Retinal pericytes isolated from 3 months DM SD rat (RtPC) retained elevated level of apoptosis when cultured either in LG or HG condition as compared to NDM animals (Supplementary Fig. 4c online). Incubating pericytes in HG or H+L condition increased expression of cleaved caspase-3 and BAX while decreasing the expression of anti-apoptotic protein Bcl-2 as compared to LG level (Supplementary Fig. 4d online). PDGF-BB increased DNA synthesis by 2.5-fold ($P < 0.01$) in BRPC at LG levels, which was inhibited > 100% when pericytes were exposed to HG conditions for 3 days (Supplementary Fig. 4e online). *In situ* total PKC activity or PKCδ activity increased by 2-fold and 30%, respectively ($P < 0.05$) in a time-dependent manner after 72 hours of exposure to HG and remained elevated after reducing glucose level to 5.6 mM (Fig. 2b and Supplementary Fig. 5a online). Immunoblot analyses showed that PKCδ was translocated from cytosol to membrane fraction when pericytes were incubated with HG (39%, $P < 0.05$) even after returning to LG concentration (Fig. 2c).

Total DAG level, an activator of PKCs, increased by 2.3-fold ($P < 0.05$) in BRPC exposed to HG for 72 hours (Fig. 2d). In contrast to PKC activation, reduction of glucose concentration to 5.6mM from 20mM reversed > 100% the increase in DAG levels (Fig. 2d). Although the half-life of PKCδ mRNA using actinomycin D was not affected in HG compared to LG, PKCδ mRNA levels increased by 2.7-fold ($P < 0.05$) when pericytes were exposed to HG, which was not reversed by changing to LG (Supplementary Fig 5b,c online). To define the causal role of PKCδ in pericyte apoptosis and the inhibition of PDGF-B actions, BRPC were transfected with adenoviral vector containing either dominant negative

(Ad-dn) or wild-type (Ad-wt) PKCδ isoform. Pericytes overexpressing GFP-control responded similarly as non-transfected cells to HG with 2-fold increase of DNA fragmentation ($0.001 < P < 0.05$) (Fig. 2e). Overexpression of Ad-wtPKCδ, but not Ad-wtPKCβ, increased DNA fragmentation by 30% and 50% ($P < 0.05$) at LG and HG conditions, respectively, whereas Ad-dnPKCδ overexpression prevented HG actions (Fig. 2e and Supplementary Fig. 5d online). Moreover, brain pericytes (BrPC) isolated from DM *Prkcd*$^{-/-}$ mice did not display increased DNA fragmentation as compared to BrPC isolated from DM *Prkcd*$^{+/+}$ mice (Supplementary Fig. 5e online). In LG condition, PDGF-BB activated ERK and Akt phosphorylation by 3 and 4-fold ($P < 0.001$), respectively (Fig. 2f). These effects of PDGF-BB were impaired by 79–100% and 67–100% in Ad-GFP and Ad-wtPKCδ infected pericytes when exposed to HG as compared to LG condition, respectively, which were completely restored in Ad-dnPKCδ overexpressed cells (Fig. 2f).

p38α MAPK isoform serves as a target for PKCδ action

Since p38 MAPK induced by activation of PKCδ can cause cellular apoptosis, [5, 16] we explored its unknown role for inhibition of PDGF signaling. HG induced p38 MAPK phosphorylation in BRPC by 2.8-fold ($P < 0.001$), which was not reversed by the additional 72 hours exposure in LG (Fig. 3a). Inhibition of p38 MAPK by SB203580 prevented HG-induced pericyte apoptosis, inhibition of DNA synthesis and Akt/ERK phosphorylation, and restored PDGF-BB actions (Fig 3b and Supplementary Fig. 6a,b online). Amongst the p38 MAPK family, α and β isoforms were mainly expressed in pericytes. Immunoprecipitation studies in pericytes exposed to LG, HG and HG+LG demonstrated that only p38α, but not p38β isoform, was increased by HG condition (Supplementary Fig. 6c online). Overexpression of Ad-dnp38α MAPK prevented completely ($P < 0.01$) HG's action on pericyte apoptosis (Fig. 3c) and reversed HG-induced inhibition of PDGF-BB action on Akt and ERK phosphorylation (Fig. 3d). Interestingly, overexpression of Ad-dnp38β MAPK exacerbated HG's actions on pericyte apoptosis and had no effect on PDGF-BB signaling inhibition (Fig. 3c,d). Since reactive oxygen species (ROS) can also be increased by hyperglycemia and cause cellular apoptosis, [17] BRPC exposed to HG condition increased ROS production by 11% ($P < 0.05$) which was not reversed by lowering glucose level to 5.6 mM (Fig. 3e). However, treatment with *N*-acetylcysteine (NAC) only partially prevented HG-induced pericyte apoptosis by 47% ($P < 0.05$) but completely prevented H_2O_2 induced cellular apoptosis (Fig. 3f).

SHP-1 in mediating PKCδ and p38α MAPK actions on PDGFR-β

A mechanism for the activated PKCδ/p38α MAPK to de-phosphorylate PDGFR-β is not known. We evaluated SHP-1 which can bind to PDGFR-β and inhibit its activation. [12] HG increased SHP-1 expression by 81% ($P < 0.01$), which remained persistently elevated when glucose levels were returned to 5.6 mM without affecting other PTPs such as SHP-2 and PTP1B or lipid phosphatase such as PTEN in BRPC (Fig. 4a). Interestingly, RtPC isolated from DM rats had significantly elevated PKCδ, p38 MAPK phosphorylation and SHP-1 expressions as compared to NDM animals either in LG or HG condition (Fig. 4b). In parallel, PKCδ and SHP-1 mRNA expression were also increased in RtPC by 73% and 78%, respectively, but not in RtEC from DM animals as compared to NDM, whereas ET-1 mRNA expression was elevated in both cell types by diabetes (Supplementary Fig. 7a online). The specific role of PKCδ and p38 MAPK activation on SHP-1 expression by HG was determined since SB203580 or Ad-dnPKCδ overexpression completely prevented HG-induced SHP-1 protein expression ($P < 0.05$) (Fig. 4c and Supplementary Fig. 7b online). Interestingly, exposure to HG level in retinal EC, BRPC overexpressing Ad-wtPKCβ or the addition of H_2O_2 (100 μM) did not increase SHP-1 expression as compared to their respective controls (Supplementary Fig. 7c–e online). SHP-1 phosphatase activity increased by 57% ($P < 0.01$) with HG exposure and not reversed by returning glucose concentration to

5.6 mM (Supplementary Fig. 8a online), but was reduced by 77% ($P < 0.01$) or 86% ($P < 0.05$), respectively in cells treated with SB203580 (Supplementary Fig. 8Aonline) or overexpressing Ad-dnPKCδ (Fig. 4d). Overexpression of Ad-dnSHP-1, knock-down SHP-1 or PKCδ with siRNA in the pericytes not only completely inhibited HG-induced pericyte apoptosis but also restored anti-apoptotic and signaling actions of PDGF-BB as compared to Ad-*LacZ* transfected cells (Fig. 4e–g and Supplementary Fig. 8b online). Our data also showed that HG condition increased cleaved caspase-8, and the overexpression of either Ad-dnPKCδ or Ad-dnSHP-1 in pericytes prevented these effects of HG (Supplementary Fig. 8c online). These results may in part explain why inhibition of PKCδ/p38α MAPK/SHP-1 pathway in culture cells can reduce pericyte apoptosis in absence of PDGF. Phosphorylation of PKCδ, p38 MAPK and expression of SHP-1 were also increased in BrPC isolated from DM as compared to NDM $Prkcd^{+/+}$ mice but not in DM $Prkcd^{-/-}$ mice (Fig. 4h). SP1 element is present in the promoter region of SHP-1. [18] We designed specific oligonucleotides of SP1 sequence (GC box) located in the bovine SHP-1 promoter region to measure SP1 transcriptional binding activity. The data showed that exposure to HG increased SP1 binding activity which can be suppressed by a SP1 inhibitor (Mithramycin A), mutated oligonucleotides in the GC box sequence or with 10-fold higher concentration of the competitor (Fig 4i). SP1 binding activity was also elevated in Ad-GFP and Ad-wtPKCδ but not in Ad-dnPKCδ overexpressed cells after HG exposure (Fig. 4j). Furthermore, to confirm that hyperglycemia promoted SHP-1 expression via SP1 transcription activity, BRPC were treated with Mithramycin A which prevented HG-induced SHP-1 expression as compared to vehicle (methanol) or untreated cells (Supplementary Fig. 8d online).

SHP-1 expression is independent of NF-κB activation

Activation of NF-κB has been reported to be involved in pericyte apoptosis induced by hyperglycemia. [19] Therefore, we evaluated the relationship between PKCδ/p38α MAPK/SHP-1 activation and NF-κB transcription activity. HG exposure increased transcriptional activity of NF-κB in Ad-GFP and Ad-wtPKCδ overexpressing cells by 3 and 4-fold ($P < 0.001$) respectively, but it was completely inhibited in Ad-dnPKC δ overexpressing pericytes (Fig. 5a). NAC treatment also completely prevented NF-κB transcriptional binding activity induced by both HG and H_2O_2 condition in BRPC (Supplementary Fig. 9 online). Further, inhibition of p38 MAPK by SB203580 (10 μM) also prevented HG-induced NF-κB transcription activity ($P < 0.001$) (Fig. 5b). Selective inhibitors of NF-κB translocation to the nucleus (SN50) or DNA binding (SM7368) partially reduced HG-induced DNA fragmentation by 60% and 52% ($P < 0.01$), respectively (Fig. 5c). However, these compounds did not reverse the inhibitory actions of HG on PDGF's anti-apoptotic effects or its signaling on the phosphorylation of ERK, Akt and tyrosine residues of PDGFR-β in BRPC (Fig. 5c,d). The inhibition of NF-κB with either SN50 or SM7368 also did not prevent HG-induced increases in SHP-1 expression (Fig. 5e).

SHP-1 and p38α MAPK are abolished in Prkcd$^{-/-}$ mice

The expression of SHP-1 was assessed in several relevant tissues including the retina and renal cortex in diabetic state. The protein expression of SHP-1 increased in the retina by 1.8 to 2-fold ($P < 0.05$) after 3, and 6 months of DM, and in the renal cortex by 1.8-fold ($P < 0.05$) after 3 months of DM (Fig. 6a,b). Using laser micro-dissection, diabetes increased SHP-1 expression in the RPE by 4-fold ($P = 0.05$) and vascular tissues by 2.1-fold ($P = 0.03$), but not in the neuronal layers (Fig. 6c). We also evaluated the role of PKCδ and reversibility of SHP-1 mRNA expression in the retina. Expression of SHP-1 mRNA increased in the retina of DM $Prkcd^{+/+}$ mice after 6 months of diabetes (4-fold; $P < 0.001$) and surprisingly remained elevated even after achieving euglycemia in the second 3-month period, but was not affected in DM $Prkcd^{-/-}$ mice as compared to NDM controls (Fig. 6d).

Both SHP-1 and phospho-p38 MAPK protein expression were elevated by 51% and 50% ($P < 0.01$), respectively, in the retina of DM *Prkcd*$^{+/+}$ mice and also those treated with insulin implants as compared to NDM *Prkcd*$^{+/+}$ mice (Fig. 6e). In contrast, DM *Prkcd*$^{-/-}$ mice displayed no changes in SHP-1 or phospho-p38 MAPK protein expression as compared to NDM *Prkcd*$^{-/-}$ mice (Fig. 6e). Immunostaining showed that pericytes (NG2) in the retinal microvessels of DM animals displayed higher fluorescence intensity for PKCδ and SHP-1 as compared to microvessel pericytes from NDM mice. In contrast, no apparent differences in fluorescence of PKCδ or SHP-1 were found in EC (isolectin B4) from NDM and DM mice (Fig. 6f). Diabetes has been associated with elevated oxidative stress marker and degradation of IkBα subunit, an indicator of increased NK-κB activity. Although cytosolic super oxide dismutase (SOD1) transgenic DM mice have reduced oxidative stress marker (data not shown) and unchanged protein expression of IkBα as compared to wild-type DM mice, these DM SOD1 transgenic mice exhibited increased SHP-1 expression by 87% ($P < 0.05$) as compared to NDM TG SOD1 mice, similarly to wild-type NDM and DM mice (Fig. 6g).

DISCUSSION

We have identified a series of common biochemical steps which are induced by hyperglycemia to activate NF-κB and PDGF-B resistance pathways to cause pericyte apoptosis, the most specific vascular histopathology associated with diabetic complications. These results showed that hyperglycemia activated PKCδ in a persistent manner probably via an increase in transcription process, which differentiates from previous reports that HG increased PKCβ in the EC. The difference between PKC isoform being activated by HG in the pericyte and EC is very important since PKCδ activation is associated with cellular apoptosis and PKCβ is known to enhance cellular growth. [14, 20] Thus, sustained increased PKCδ levels for several months of diabetes correlated closely with the appearance of retinal pericyte apoptosis/acellular capillaries after 5–6 months of diabetes, which was not reversed with re-establishment of normoglycemia. In contrast, activation of PKCβ isoform in the EC mediates increases in ET-1 expression and enhances VEGF action to cause endothelial dysfunction and decrease RBF. [21, 22] Clinical trials using PKCβ selective inhibitor delayed the loss of visual acuity and progression of diabetic macular edema, but did not affect the progression of proliferative DR, [23] suggesting more than PKCβ activation is involved in the vascular pathology of DR. The present study shows that hyperglycemia activates PKCδ, but not PKCβ, specifically in the pericytes and leading to its apoptosis is supported by multiple lines of evidence using immunohistochemistry of the microvessels, retinal pericytes isolated from diabetic rats and by the resistance of DM *Prkcd*$^{-/-}$ mice to develop pericyte loss, acellular capillaries, and retinal permeability as compared to DM *Prkcd*$^{+/+}$ mice. The *in vivo* studies confirmed that PKCδ activation led to PDGF resistance in the retina of DM PKCδ$^{+/+}$ mice, a finding not observed in *Prkcd*$^{-/-}$ mice. Moreover, the specific inhibition of PKCδ in pericytes, either by *in vitro* or *Prkcd*$^{-/-}$ mice *in vivo* also prevented SHP-1 expression and NF-κB activation, strongly indicating PKCδ actions are upstream to both pathways. These findings clearly identify the pivotal role for PKCδ activation as a cause of pericyte apoptosis and acellular capillaries. Multiple stimuli have been reported to increase PKCδ activation or transcription rate, including oxidative stress, UV and other stresses. [24] In the present study, activation of PKCδ and its elevated level of protein persist in pericytes cultured from diabetic animals even when hyperglycemic stimuli have been reversed. Our data suggest that chronic activation of PKCδ is most likely by transcription rather than activation since increases in DAG levels are not maintained after the reversal of HG to LG conditions. However, it is possible that local and transient production of DAG levels may be sufficient to maintain PKC activity. In addition, HG appears to increase the transcription rate of PKCδ since the protein expression of PKCδ increases without parallel changes in the half-life of PKCδ mRNA. The persistent elevation of PKCδ in pericytes could be similar to the reported

epigenetic modification of histone methylation to explain persistent activation of NF-κB induced by hyperglycemia in monocytes, endothelial and smooth muscle cells. [25–27] Our results do not provide mechanisms to explain the persistent elevation of PKCδ.

One specific target of PKCδ to induce cellular apoptosis appears to be p38α MAPK isoform but not p38β MAPK. Several mechanisms could explain the activation of p38α MAPK by PKCδ, including direct activation, changes in p53 protein and possibly indirectly by activation of MEK. [15] Our results are consistent with previous studies that have shown p38α MAPK can be used as pro-apoptotic marker whereas p38β MAPK has been mainly associated with migration, transcriptional regulation of Bcl-2 and anti-apoptotic effects. [28, 29]

Our results showed that the activation of PKCδ/p38α MAPK stimulation induced by HG can cause pericyte apoptosis through two different pathways: ROS/NF-κB activation and deactivation of PDGFR-β on Akt or ERK phosphorylation. Activation of p38α MAPK via NF-κB and the caspase pathway to cause apoptosis mediated by HG has been reported. [19] Previous studies and our data using SOD transgenic mice support evidence that oxidative stress induces NF-κB pathway, which can cause pericyte apoptosis. However, our results showed that treatment with two inhibitors of NF-κB and antioxidant only partially inhibited HG-induced pericyte apoptosis and did not prevent HG-induced inhibition of PDGF-BB's actions on Akt or ERK activation. In contrast, inhibition of PKCδ and p38α MAPK was able to prevent completely HG or diabetes-induced pericyte apoptosis. These results suggest that HG can induce pericyte apoptosis at steps downstream of p38α MAPK activation, partially via the known NF-κB cascade and, equally, via an independent pathway, which induces apoptosis through the inhibition of PDGF actions.

Our findings have identified SHP-1 as a novel downstream target of PKCδ/p38α MAPK. SHP-1 has been reported to down regulate several receptor tyrosine kinases, including PDGFR-β, insulin, EGF and VEGFR-2. [12, 13, 30, 31] However, regulation of SHP-1 by HG and by p38 MAPK have not been reported. *in vivo* mice deficient of SHP-1 due to mutation have severe hematopoietic disruption leading to patch dermatitis, extramedullary hematopoiesis, splenomegaly and hemorrhagic pneumonitis resulting in death after several weeks. [32, 33] Therefore, evaluation of SHP-1 depletion after 6 months of diabetes in mice was impossible. SHP-1 may have direct effects on the retina given that SHP-1 deficient mice exhibit retinal photoreceptor dysfunction. [34] Interestingly, our results using dominant-negative or siRNA of SHP-1 completely prevented or reversed HG/PKCδ/p38α MAPK-induced inhibition of PDGF's activation and apoptosis in the pericytes. These results have identified SHP-1 for the first time as a cellular target of p38α MAPK to induce apoptosis via SP1 transcriptional activity by de-activating essential survival action of receptor's growth factors such as PDGFR-β, an NF-κB independent pathway. The results from cultured pericytes derived from diabetic animals, retinal laser micro-dissection and immunohistochemistry analysis indicated that the changes in SHP-1 expression are sustained and tissue selective, potentially involved in other tissues in diabetes besides pericytes such as RPE and perivascular cells (glia cells) in the retina and even renal podocytes. These findings support the idea that HG-induced PKCδ and SHP-1 activation could cause cellular apoptosis, a common cellular feature of diabetic vascular complications involving the retina, renal glands, and cardiovascular tissue. The importance of PKCδ in pericyte apoptosis was demonstrated using DM *Prkcd*$^{-/-}$ mice which are resistance to acellular capillaries. However, analyses of acellular capillaries and pericyte ghosts are morphological measures that imply the absence of pericytes after trypsin digestion and cannot definitively demonstrate the cell type or mechanism of cell death.

In summary, this study documented that hyperglycemia persistently activated a novel signaling cascade and molecular target of PKCδ/p38α MAPK, SHP-1, to cause pericyte apoptosis in cultured cells and *in vivo* to initiate DR. Our data demonstrated that HG can activate PKCδ/p38α MAPK to induce two independent pathways of NF-κB-activation and SHP-1/PDGFR-β deactivation to promote pericyte apoptosis and acellular capillaries. These findings have identified several potential new therapeutic targets for the treatment of retinopathy and potentially other vascular complications of diabetes.

METHODS

Animal and experimental design

Prkcd$^{-/-}$ mice were produced as described previously and provided by Dr. Michael Leitges. [35] *Prkcd*$^{-/-}$ mice with mixed background of 129SV and C57BL/6J strains were crossbred eight generations (F8) with wild-type C57BL/6J background from Jackson Laboratory. SOD1 transgenic mice were purchased from Jackson Laboratory. *Prkcd*$^{-/-}$, SOD1 transgenic and their age-matched control mice were used at 7–8 weeks of age. Animals were rendered diabetic by streptozotocin (STZ) (Sigma) (90 mg kg^{-1} in 0.05 M citrate buffer, pH. 4.5, i.p.) on two consecutive days after overnight fast; control mice were injected with citrate buffer. After three months of diabetes, animals received insulin implants (Linbit, LinShin Canada) subcutaneously to normalize blood glucose level. Male SD rats were obtained from Charles River Laboratories. All experiments followed the guidelines of the Association for Research in Vision and Ophthalmology and were approved by the Animal Care and Use Committees of the Joslin Diabetes Center, according to NIH guidelines.

Blood glucose and insulin levels

Blood glucose was measured by Glucometer (Elite, Bayer Inc). Plasma insulin levels were measured using sensitive rat insulin ELISA kit (Crystal Chem Inc) according to the manufacturer's instructions.

Quantitation of pericyte loss

The retinal vasculature was isolated by the trypsin digest method previously described and air-dried onto glass slides. Sections were then stained with hematoxylin and periodic acid–Schiff, dehydrated, and coverslipped. [36] Pericyte ghosts were estimated from the prevalence of protruding "bumps" in the capillary basement membranes from which pericytes had disappeared. Acellular capillaries were quantitated in four to seven field areas in the mid-retina (200x magnification) in a masked manner. Acellular capillaries were identified as capillary-sized vessel tubes having no nuclei anywhere along their length including or not vessel "strands" and were reported per square millimeter of retinal area. At least 1,000 capillary cells (endothelial cells and pericytes) in five field areas in the mid-retina (400x magnification) in a masked manner were examined. Pericyte loss was quantified by the combined number of pericyte ghosts and acellular capillaries.

Cell culture

Fresh calf eyes were obtained from a local abattoir. Primary cultures of mouse brain (BrPC), rat retinal pericytes (RtPC) and endothelial cells (RtEC), and bovine retinal pericytes (BRPC) and endothelial cells (BREC) were isolated by homogenization and a series of filtration steps as described previously. [37] BREC and RtEC were subsequently propagated with DMEM and 10% FBS, 100 μg ml^{-1} heparin, and 50 μg ml^{-1} endothelial cell growth factor (Roche Applied Science) and grown on collagen I-coated dishes (BD Biosciences). BRPC, BrPC and RtPC were cultured in DMEM and 20% FBS. Pericytes were

characterized for homogeneity by immunoreactivity with monoclonal antibody 3G5. [38] Cells from passages 2 through 5 were used in these experiments. Cells were exposed to 5.6 mM of glucose (LG) or to addition 20 mM of glucose (HG) for 72 hours or 6 days and returned to LG for an extended period of 72 hours (H+L) in low serum condition (1%). The osmotic pressure was adjusted by adding proper concentration of mannitol in LG condition.

Measurement of DAG concentrations

Total DAG levels were measured with a radioenzymatic assay kit (Amersham Corp.) using DAG kinase that quantitatively converts DAG to [^{32}P] phosphatidic acid (PA) in the presence of [γ-^{32}P]-ATP (New England Nuclear). The values of total DAG contents were normalized by the amount of cellular proteins.

Immunohistochemistry

Retinal microvessels from NDM and DM mice were isolated and fixed with 4% paraformaldehyde for 1 hour on a cover slip. Tissues were blocked with 10% goat serum for 1 hour, exposed in sequence to primary antibodies (NG2, Isolectin B4-coupled with FITC and PKCδ or SHP-1, 1:100) over night following by incubation with secondary antibodies dylight-649 conjugated anti-mouse IgG (Jackson ImmunoResearch Laboratories; 1:500) or 7-amino-4-methylcoumarin-3-acetic acid (AMCA)-conjugated anti-rabbit IgG (Abcam, 1:500). Confocal images were captured on a Zeiss LSM 410 microscope; images of 1 experiment were taken at the same time under identical settings and handled in Adobe Photoshop similarly across all images.

Phosphatase assay

We assessed phosphatase activity of SHP-1 by using the RediPlate 96 EnzChek Tyrosine Phosphatase Assay kit (Invitrogen) according to the manufacturer's instructions. W e immunoprecipitated SHP-1 from cell and tissue lysates with a polyclonal antibody (Santa Cruz Laboratories, clone C19) prebound to protein A Sepharose beads. After overnight incubation, we washed beads three times with PBS containing 1% Igepal CA-630 and 5 mM dithiothreitol (DTT). We placed beads into RediPlate wells and incubated them for 30 min at 20–22 °C before reading them for fluorescence.

Adenoviral Vector Transfection

Adenoviral vectors containing green fluorescent protein (GFP, Ad-GFP), *LacZ* (Ad-*LacZ*) and dominant negative or wild-type PKCδ isoforms (Ad-dnPKCδ and Ad-wtPKCδ) were constructed and used to infect pericytes as we have reported previously in various vascular cells and pancreatic cells. [39, 40] Adenoviral vector of dominant negative p38α and β MAPK were generously gifted by Y.Wang as prepared as previously described. [41] Adenoviral vector of dominant negative of SHP-1 (Ad-dnSHP-1) was generously provided by A. Marette and prepared as previously described. [13] Description of the infection methods is described in Supplementary Methods online.

Statistical analysis

The data were shown as mean ± SD for each group. Statistical analysis was performed by unpaired *t* test or by one-way analysis of variance (ANOVA) followed by Tukey's test correction for multiple comparisons. All results were considered statistically significant at $P < 0.05$.

Other methods

Measurement of PKC activity assay, laser capture micro dissection, intracellular ROS production, nuclear extract and NoShift transcription factor assay, immunoblot analyses, real

time PCR analysis, adenoviral vector transfection, DNA fragmentation and synthesis analysis, measurement of mean circulation time (MCT), retinal blood flow (RBF), retinal permeability and vascular permeability with Evans blue dye, and reagents and antibodies are described in Supplementary Methods online.

Supplementary Material

Refer to Web version on PubMed Central for supplementary material.

Acknowledgments

P. Geraldes is a recipient of awards from the Juvenile Diabetes Research Foundation. This study was supported by National Eye Institute (grant 5R01EY016150-02) to G.L. King, and by the CIHR (grant #165453) to A. Marette. We thank W-C. Li and S. Bonner-Weir for the technical support on confocal microscopy imaging.

References

1. Lorenzi M, Gerhardinger C. Early cellular and molecular changes induced by diabetes in the retina. Diabetologia. 2001; 44:791–804. [PubMed: 11508263]
2. Isermann B, et al. Activated protein C protects against diabetic nephropathy by inhibiting endothelial and podocyte apoptosis. Nature medicine. 2007; 13:1349–1358.
3. >The effect of intensive treatment of diabetes on the development and progression of long-term complications in insulin-dependent diabetes mellitus. The Diabetes Control and Complications Trial Research Group. N Engl J Med. 1993; 329:977–986. [PubMed: 8366922]
4. Mizutani M, Kern TS, Lorenzi M. Accelerated death of retinal microvascular cells in human and experimental diabetic retinopathy. J Clin Invest. 1996; 97:2883–2890. [PubMed: 8675702]
5. Busik JV, Mohr S, Grant MB. Hyperglycemia-induced reactive oxygen species toxicity to endothelial cells is dependent on paracrine mediators. Diabetes. 2008; 57:1952–1965. [PubMed: 18420487]
6. Hammes HP. Pericytes and the pathogenesis of diabetic retinopathy. Hormone and metabolic research = Hormon- und Stoffwechselforschung = Hormones et metabolisme. 2005; 37 Suppl 1:39–43. [PubMed: 15918109]
7. Sustained effect of intensive treatment of type 1 diabetes mellitus on development and progression of diabetic nephropathy: the Epidemiology of Diabetes Interventions and Complications (EDIC) study. Jama. 2003; 290:2159–2167. [PubMed: 14570951]
8. Kuwabara T, Cogan DG. Retinal vascular patterns. VI. Mural cells of the retinal capillaries. Arch Ophthalmol. 1963; 69:492–502. [PubMed: 13927676]
9. Frank RN. Diabetic retinopathy. N Engl J Med. 2004; 350:48–58. [PubMed: 14702427]
10. Enge M, et al. Endothelium-specific platelet-derived growth factor-B ablation mimics diabetic retinopathy. The EMBO journal. 2002; 21:4307–4316. [PubMed: 12169633]
11. Yokota T, et al. Role of protein kinase C on the expression of platelet-derived growth factor and endothelin-1 in the retina of diabetic rats and cultured retinal capillary pericytes. Diabetes. 2003; 52:838–845. [PubMed: 12606528]
12. Yu Z, et al. SHP-1 associates with both platelet-derived growth factor receptor and the p85 subunit of phosphatidylinositol 3-kinase. The Journal of biological chemistry. 1998; 273:3687–3694. [PubMed: 9452499]
13. Dubois MJ, et al. The SHP-1 protein tyrosine phosphatase negatively modulates glucose homeostasis. Nature medicine. 2006; 12:549–556.
14. Koya D, King GL. Protein kinase C activation and the development of diabetic complications. Diabetes. 1998; 47:859–866. [PubMed: 9604860]
15. Ryer EJ, et al. Protein kinase C delta induces apoptosis of vascular smooth muscle cells through induction of the tumor suppressor p53 by both p38-dependent and p38-independent mechanisms. The Journal of biological chemistry. 2005; 280:35310–35317. [PubMed: 16118209]

16. Igarashi M, et al. Glucose or diabetes activates p38 mitogen-activated protein kinase via different pathways. J Clin Invest. 1999; 103:185–195. [PubMed: 9916130]
17. Brownlee M. Biochemistry and molecular cell biology of diabetic complications. Nature. 2001; 414:813–820. [PubMed: 11742414]
18. Nakase K, Cheng J, Zhu Q, Marasco WA. Mechanisms of SHP-1 P2 promoter regulation in hematopoietic cells and its silencing in HTLV-1-transformed T cells. Journal of leukocyte biology. 2009; 85:165–174. [PubMed: 18948549]
19. Romeo G, Liu WH, Asnaghi V, Kern TS, Lorenzi M. Activation of nuclear factor-kappaB induced by diabetes and high glucose regulates a proapoptotic program in retinal pericytes. Diabetes. 2002; 51:2241–2248. [PubMed: 12086956]
20. Idris I, Gray S, Donnelly R. Protein kinase C activation: isozyme-specific effects on metabolism and cardiovascular complications in diabetes. Diabetologia. 2001; 44:659–673. [PubMed: 11440359]
21. Ishii H, et al. Amelioration of vascular dysfunctions in diabetic rats by an oral PKC beta inhibitor. Science. 1996; 272:728–731. [PubMed: 8614835]
22. Aiello LP, et al. Vascular endothelial growth factor in ocular fluid of patients with diabetic retinopathy and other retinal disorders. N Engl J Med. 1994; 331:1480–1487. [PubMed: 7526212]
23. The effect of ruboxistaurin on visual loss in patients with moderately severe to very severe nonproliferative diabetic retinopathy: initial results of the Protein Kinase C beta Inhibitor Diabetic Retinopathy Study (PKC-DRS) multicenter randomized clinical trial. Diabetes. 2005; 54:2188–2197. [PubMed: 15983221]
24. Kanthasamy AG, Kitazawa M, Kanthasamy A, Anantharam V. Role of proteolytic activation of protein kinase Cdelta in oxidative stress-induced apoptosis. Antioxidants & redox signaling. 2003; 5:609–620. [PubMed: 14580317]
25. Miao F, et al. Genome-wide analysis of histone lysine methylation variations caused by diabetic conditions in human monocytes. The Journal of biological chemistry. 2007; 282:13854–13863. [PubMed: 17339327]
26. El-Osta A, et al. Transient high glucose causes persistent epigenetic changes and altered gene expression during subsequent normoglycemia. The Journal of experimental medicine. 2008; 205:2409–2417. [PubMed: 18809715]
27. Villeneuve LM, et al. Epigenetic histone H3 lysine 9 methylation in metabolic memory and inflammatory phenotype of vascular smooth muscle cells in diabetes. Proceedings of the National Academy of Sciences of the United States of America. 2008; 105:9047–9052. [PubMed: 18579779]
28. Peter PS, et al. Inhibition of p38 alpha MAPK rescues cardiomyopathy induced by overexpressed beta 2-adrenergic receptor, but not beta 1-adrenergic receptor. J Clin Invest. 2007; 117:1335–1343. [PubMed: 17446930]
29. Nemoto S, Xiang J, Huang S, Lin A. Induction of apoptosis by SB202190 through inhibition of p38beta mitogen-activated protein kinase. The Journal of biological chemistry. 1998; 273:16415–16420. [PubMed: 9632706]
30. Tenev T, et al. Both SH2 domains are involved in interaction of SHP-1 with the epidermal growth factor receptor but cannot confer receptor-directed activity to SHP-1/SHP-2 chimera. The Journal of biological chemistry. 1997; 272:5966–5973. [PubMed: 9038217]
31. Bhattacharya R, Kwon J, Wang E, Mukherjee P, Mukhopadhyay D. Src homology 2 (SH2) domain containing protein tyrosine phosphatase-1 (SHP-1) dephosphorylates VEGF Receptor-2 and attenuates endothelial DNA synthesis, but not migration*. Journal of molecular signaling. 2008; 3:8. [PubMed: 18377662]
32. Shultz LD, et al. Mutations at the murine motheaten locus are within the hematopoietic cell protein-tyrosine phosphatase (Hcph) gene. Cell. 1993; 73:1445–1454. [PubMed: 8324828]
33. Bignon JS, Siminovitch KA. Identification of PTP1C mutation as the genetic defect in motheaten and viable motheaten mice: a step toward defining the roles of protein tyrosine phosphatases in the regulation of hemopoietic cell differentiation and function. Clinical immunology and immunopathology. 1994; 73:168–179. [PubMed: 7923924]

34. Lyons BL, et al. Deficiency of SHP-1 protein-tyrosine phosphatase in "viable motheaten" mice results in retinal degeneration. Investigative ophthalmology & visual science. 2006; 47:1201–1209. [PubMed: 16505059]
35. Leitges M, et al. Exacerbated vein graft arteriosclerosis in protein kinase Cdelta-null mice. J Clin Invest. 2001; 108:1505–1512. [PubMed: 11714742]
36. Kern TS, Engerman RL. Comparison of retinal lesions in alloxan-diabetic rats and galactosefed rats. Current eye research. 1994; 13:863–867. [PubMed: 7720392]
37. King GL, Berman AB, Bonner-Weir S, Carson MP. Regulation of vascular permeability in cell culture. Diabetes. 1987; 36:1460–1467. [PubMed: 3678623]
38. Lindahl P, Johansson BR, Leveen P, Betsholtz C. Pericyte loss and microaneurysm formation in PDGF-B-deficient mice. Science. 1997; 277:242–245. [PubMed: 9211853]
39. Suzuma K, et al. Characterization of protein kinase C beta isoform's action on retinoblastoma protein phosphorylation, vascular endothelial growth factor-induced endothelial cell proliferation, and retinal neovascularization. Proceedings of the National Academy of Sciences of the United States of America. 2002; 99:721–726. [PubMed: 11805327]
40. Kaneto H, et al. Involvement of protein kinase C beta 2 in c-myc induction by high glucose in pancreatic beta-cells. The Journal of biological chemistry. 2002; 277:3680–3685. [PubMed: 11714718]
41. Wang Y, et al. Cardiac muscle cell hypertrophy and apoptosis induced by distinct members of the p38 mitogen-activated protein kinase family. The Journal of biological chemistry. 1998; 273:2161–2168. [PubMed: 9442057]

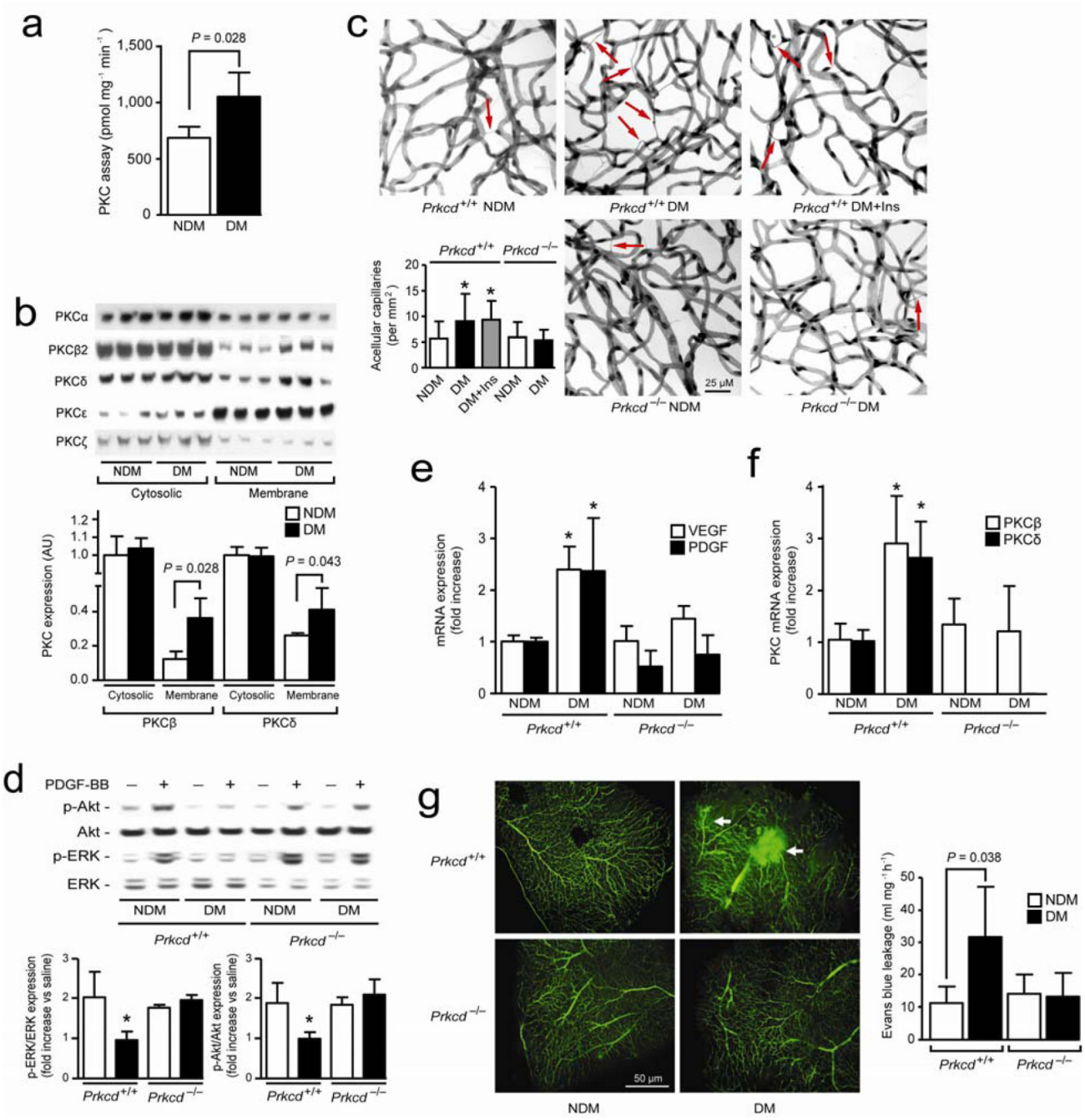

Figure 1. PKCδ activation cause PDGF-BB and microvascular abnormalities

(**a**) *In situ* PKC activity assay was measured in retina of 3 months diabetic mice (n = 6) as compared to non-diabetic mice as described in method section. (**b**) Immunoblot analyses of different PKC isoform in cytosolic and membrane fraction of retinal isolated microvessels of NDM and 3 months DM mice. (**c**) Quantification of acellular capillaries (red arrow) of *Prkcd*$^{+/+}$ and *Prkcd*$^{-/-}$ mouse retina (NDM *Prkcd*$^{+/+}$, n = 22; DM *Prkcd*$^{+/+}$, n = 19; DM+Ins *Prkcd*$^{+/+}$, n = 12; NDM *Prkcd*$^{-/-}$, n = 13; DM *Prkcd*$^{-/-}$, n = 13). (**d**) Immunoblot analyses of intravitreous injection of saline or PDGF-BB of NDM and DM mice retina. (**e**) Expression of VEGF, PDGF, (**f**) PKCβ and PKCδ mRNA from isolated microvessels of NDM and DM *Prkcd*$^{+/+}$ or *Prkcd*$^{-/-}$ mice. (**g**) Flat mount of retina infused with FITC-

dextran and permeability assay using Evans blue dye. Immunoblot experiments were done at least in triplicate. Results are shown as mean ± SD of 3–4 independent experiments * $P < 0.05$ versus NDM *Prkcd*$^{+/+}$ mice.

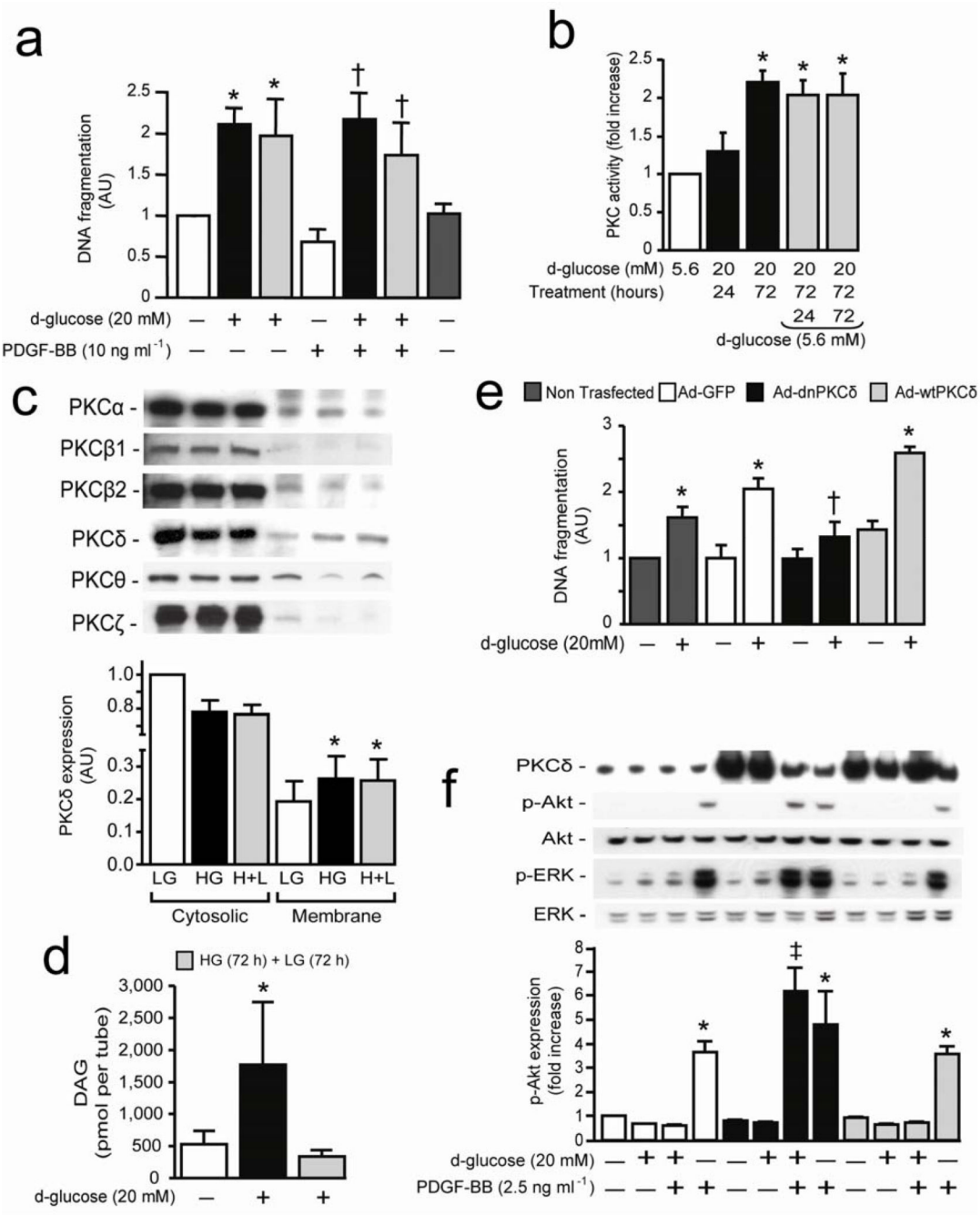

Figure 2. Hyperglycemia inhibits PDGF-B actions and induces pericyte apoptosis through activation of PKCδ isoform

(**a**) BRPC were incubated with LG (5.6 mM; white bars) or HG (20 mM; black bars) for 72 hours and then LG (gray bars) for an additional 72 hours in absence or presence of PDGF-BB. DNA fragmentation was measured according to manufacturer's instructions. (**b**) *In situ* PKC activity assay was measured in BRPC exposed to HG or LG as described in method section. (**c**) Immunoblot analyses of different PKC isoform in cytosolic and membrane fraction of BPRC. (**d**) Total DAG was measured as described in method section. (**e,f**) BRPC were transfected with Ad-GFP (white bars), Ad-dnPKCδ (black bars) or Ad-wtPKCδ (gray bars). BRPC were incubated with LG or HG for 72 hours. (**e**) DNA fragmentation was

measured according to manufacturer's instructions. (**f**F) Expression of PKCδ, phospho-ERK, ERK, phospho-Akt and Akt were detected by Western blot and densitometric quantitation was measured. Results are shown as mean ± SD of 3–5 independent experiments. * $P < 0.01$ versus LG, † $P < 0.05$ versus PDGF-BB, ‡ $P < 0.05$ versus HG.

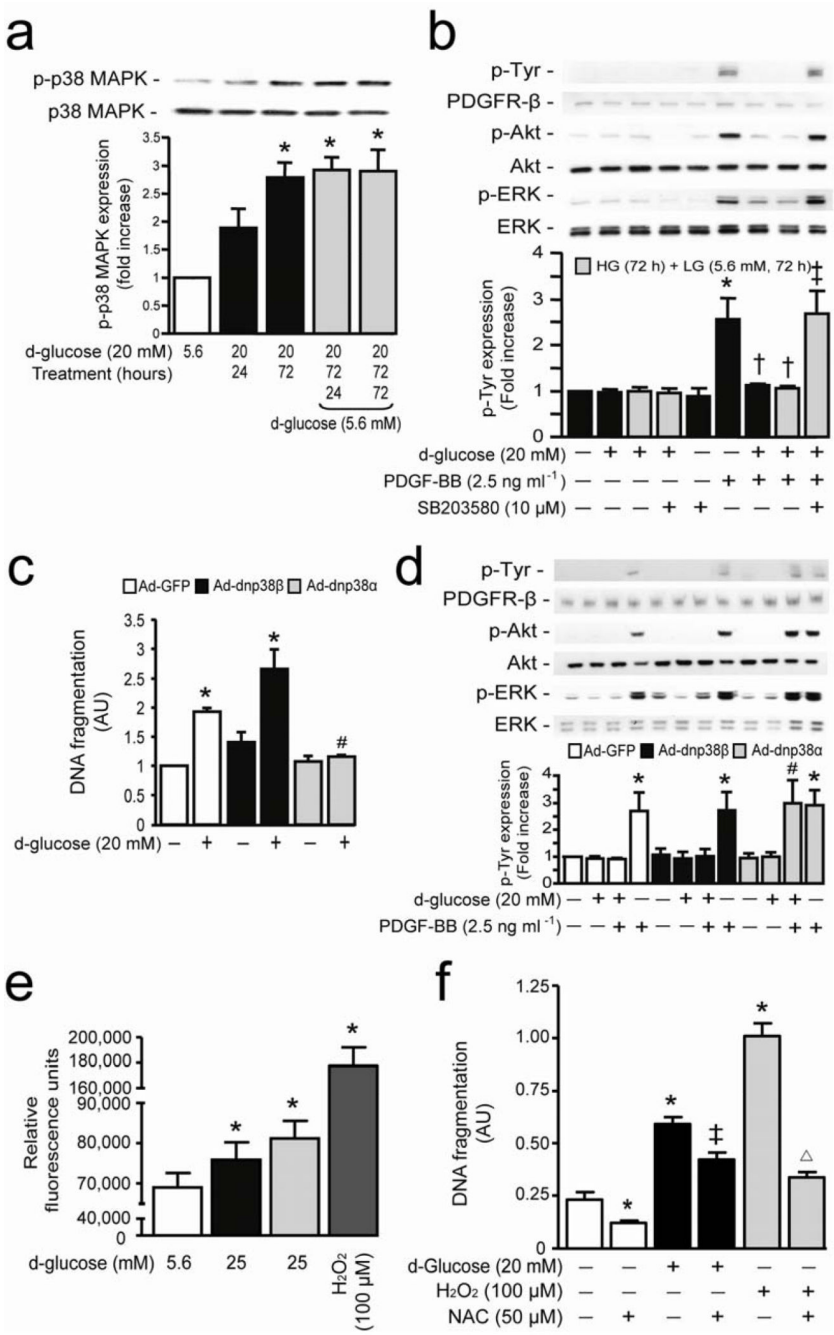

Figure 3. P38α MAPK serves as a downstream target for hyperglycemia to cause PDGF-B resistance and pericyte apoptosis

(**a**) BRPC were incubated with LG (5.6 mM; white bars) or HG (20 mM; black bars) for 24–72 hours and then LG (5.6 mM; gray bars) for an additional 24–72 hours. Expression of phospho-p38 MAPK and p38 MAPK were detected by Western blot. (**b**) Cells were exposed to LG or HG in presence or absence of SB203580 and then stimulated with PDGF-BB for 10 min. (**c**) BRPC were transfected with Ad-GFP (white bars), Ad-dnp38β MAPK (black bars) or Ad-dnp38α MAPK (gray bars), exposed to HG for 72 hours. DNA fragmentation was measured according to manufacturer's instructions. (**d**) After transfection and exposure to LG or HG for 72 hours, cells were stimulated with PDGF-BB for 10 min. (**b,d**)

Expression of phospho-Tyr, PDGFR-β, phospho-Akt, Akt, phospho-ERK were detected by Western blot and densitometric quantitation was measured. (**e**) ROS production was measured in BPRC exposed to LG, HG, H+L and H_2O_2 as described in the method section. (**f**) BPRC were exposed to LG and HG for 72 hours or H_2O_2 for 2 hours in absence or presence of NAC. DNA fragmentation was measured according to manufacturer's instructions. Results are shown as mean ± SD of 3–5 independent experiments. * $P < 0.05$ versus LG, † $P < 0.05$ versus PDGF-BB, ‡ $P < 0.05$ versus HG, # $P < 0.05$ versus HG +PDGF-BB in Ad-GFP cells, Δ $P < 0.05$ versus H_2O_2.

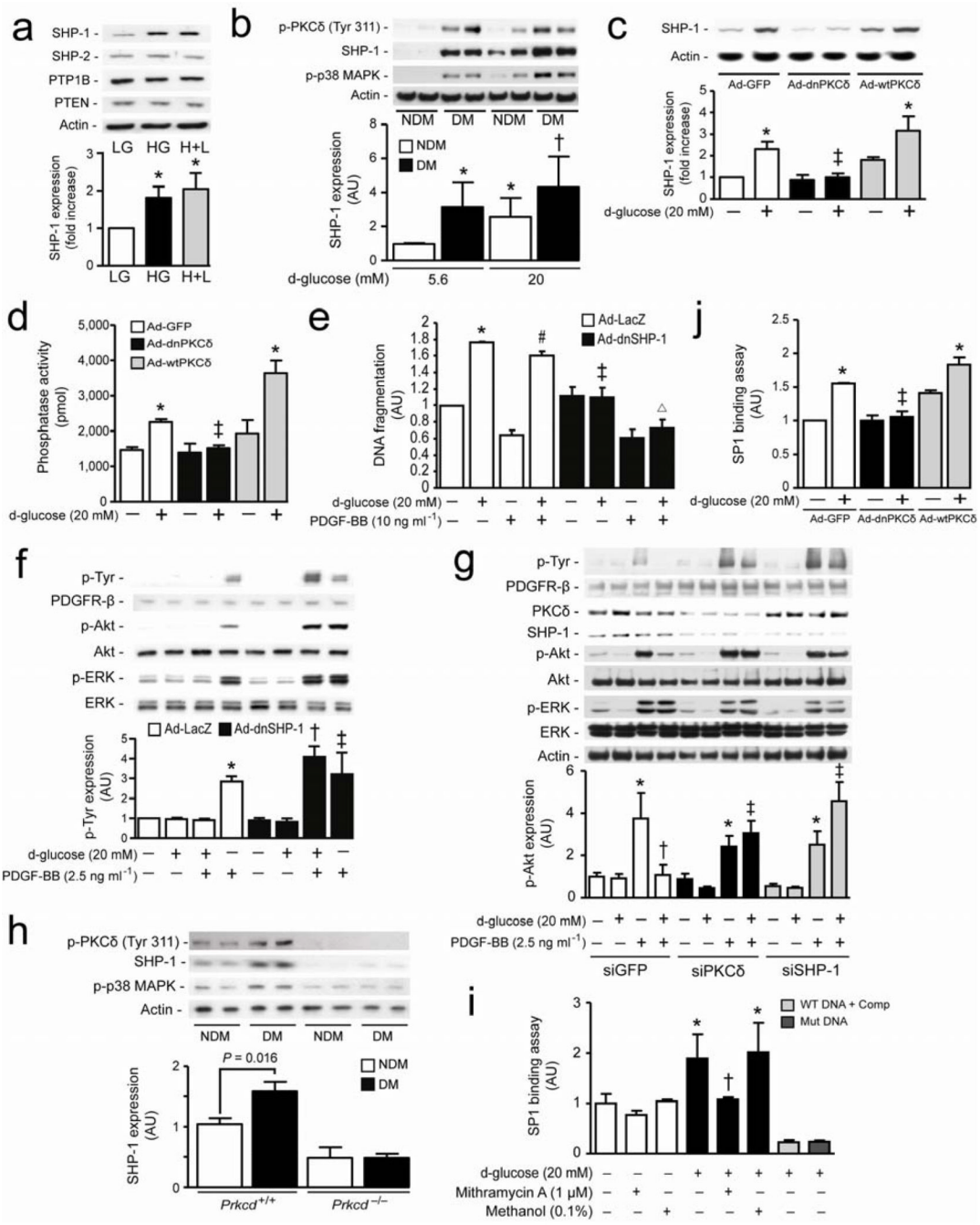

Figure 4. SHP-1 causes inhibition of PDGF signaling pathway induced by hyperglycemia and PKCδ/p38α MAPK activation

(**a**) BRPC were exposed to LG and HG as described in the method section. Expression of SHP-1, SHP-2, PTP1B, PTEN were detected by Western blot and normalized to actin expression. (**b**) RtPC isolated from NDM and DM rats cultured in LG or HG for 72 hours. (**c,d,j**) BRPC were transfected with either ad-GFP (white bars), Ad-dnPKCδ (black bars) or Ad-wtPKCδ (grey bars) and then incubated with LG or HG for 72 hours. (**d**) Phosphatase activity was measured using commercially available kit as described in the method section. (**e,f**) Cells were transfected with either Ad-LacZ (white bars) or Ad-dnSHP-1 (black bars), exposed to HG (20 mM) for 72 hours in presence or absence of PDGF-BB. (**e**) Apoptosis

was measured by DNA fragmentation according to manufacturer's instructions. (**g**) BRPC were transfected with either GFP (white bars), PKCδ (black bars) or SHP-1 (gray bars) siRNA, exposed to LG or HG for 72 hours and then stimulated with PDGF-BB. (**h**) BrPC of NDM and DM *Prkcd*$^{+/+}$ and *Prkcd*$^{-/-}$ mice were cultured in LG for 72 hours. (**i,j**) Transcriptional binding assay of SP1 was performed as described in the method section. (**i**) BRPC were exposed to LG or HG in presence or absence of mithramycin A or methanol. (**b,c,f,g,h**) Expression of phospho-Tyr, phospho-PKCδ, PDGFR-β, phospho-Akt, Akt, phospho-ERK, ERK, phospho-p38 MAPK, SHP-1 and actin were detected by Western blot and densitometric quantitation was measured. Results are shown as mean ± SD of 3–5 independent experiments. * $P < 0.05$ versus LG, † $P < 0.05$ versus HG or HG+LG, ‡ $P < 0.05$ versus HG in Ad-GFP or HG in siGFP, # $P < 0.05$ versus PDGF-BB, Δ $P < 0.05$ versus HG in Ad-dnSHP-1.

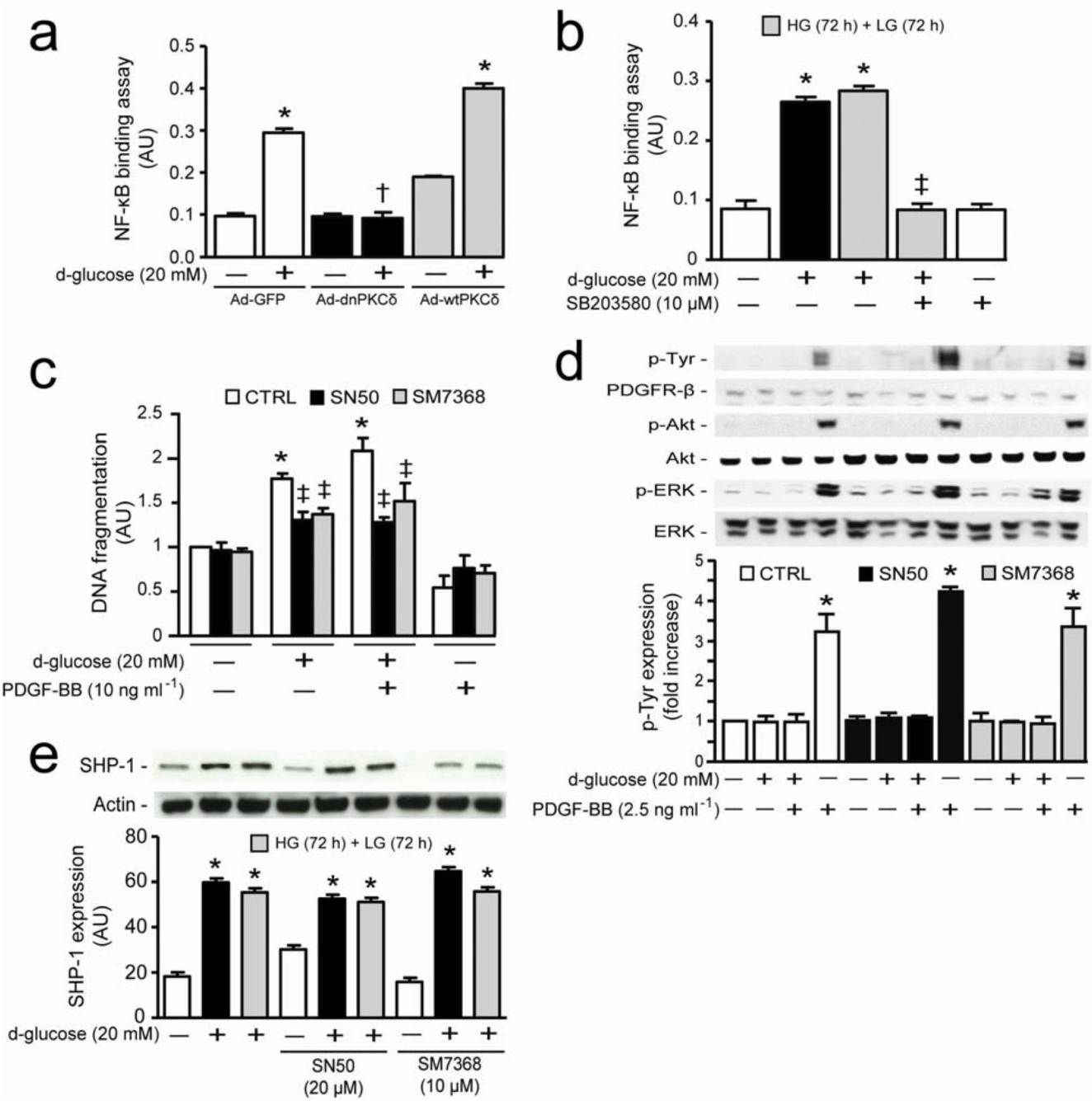

Figure 5. Increase of SHP-1 expression by hyperglycemia is independent of NF-κB activation

(A**a**) BRPC were transfected with either ad-GFP (white bars), Ad-dnPKCδ (black bars) or Ad-wtPKCδ (gray bars) and then incubated with LG or HG for 72 hours. (**b**) Transcriptional binding activity assay of NF-κB was performed as described in the method section. (**c**) BRPC were incubated with LG or HG in absence (white bars) or presence of inhibitor or NF-κB (SN50, black bars; SM7368, gray bars). Apoptosis was measured by DNA fragmentation according to manufacturer's instructions. (**d**) BRPC were incubated as described in (**c**) and then stimulated with PDGF-BB for 10 min. Expression of phospho-Tyr, PDGFR-β, phospho-Akt, Akt, phospho-ERK, ERK and (**e**) SHP-1 were detected by Western blot and densitometric quantitation was measured. Results are shown as mean ± SD of 3–5

independent experiments. * $P < 0.05$ versus LG, † $P < 0.05$ versus HG in Ad-GFP, ‡ $P < 0.05$ versus HG or HG+LG.

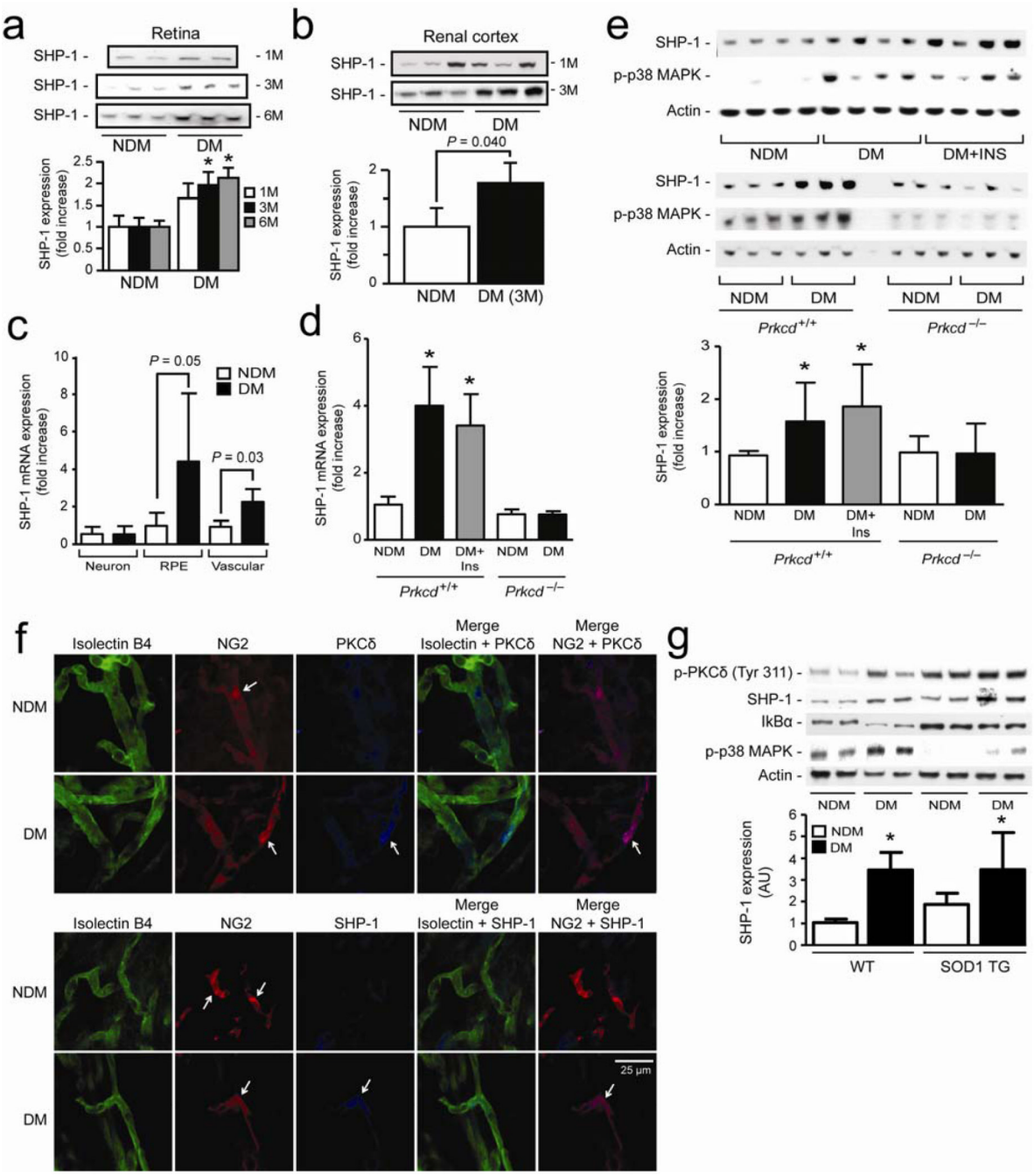

Figure 6. PKCδ induces SHP-1 expression and p38 MAPK activation in retina, kidney and PBMC of diabetic rodent animals

Expression of SHP-1 in (**a**) retina and (**b**) renal cortex of 1 to 6 months diabetic mice. (**c**) SHP-1 mRNA expression in retinal neurone, RPE and vascular of NDM and 6 month DM mice by laser capture micro-dissection as described in the method section. (**d**) SHP-1 mRNA, (**e**) SHP-1 protein expression and p38 MAPK activity in whole retina of NDM and 6 months DM *Prkcd*$^{+/+}$ and *Prkcd*$^{-/-}$ mice. (**f**) Immunofluorescence of endothelial cells (isolectin B4; green), pericytes (NG2; red) and PKCδ or SHP-1 (blue) of isolated retinal microvessels from NDM and 3 months DM mice. (**g**) SHP-1, phospho-PKCδ, phosho-p38 MAPK, IkBα and actin expression in whole retina of NDM and DM wild-type and SOD1

transgenic mice. Immunoblot analyses and densitometric quantitation were performed. Results are shown as mean ± SD of 3–5 independent experiments. * $P < 0.05$ versus NDM *Prkcd*$^{+/+}$ mice.